**Proceedings of the 7th GACM Colloquium on Computational Mechanics
for Young Scientists from Academia and Industry
October 11-13, 2017 in Stuttgart, Germany**

Computation of multiphysics processes in deformable media

Bilen Emek Abali[1]*

Micro Abstract
Micro electro-mechanical systems (MEMS) exploit the coupling between mechanics and electromagnetism. For an accurate simulation of this coupling we need a strategy to calculate deformation, temperature, and electromagnetic fields in solids, at once. By using open-source packages, we present an approach to simulate MEMS by solving nonlinear and coupled equations at once by using finite difference method in time and finite element method in space.

[1]Institute of Mechanics, Technische Universitaet Berlin, Berlin, Germany
***Corresponding author**: bilenemek@abali.org

Introduction

Micro-electro-mechanical systems (MEMS) exploit the electromagnetic interaction with elastic materials such that a deformation induces a voltage change or a magnetic field generates a deformation. A growing use is observed of such transducers transforming electromagnetic and mechanical energies into each other. The increasing number of applications is not only owing to quick and economic manufacturing possibilities but also because of the simulation methods allowing to reduce or even eliminate the testing period before mass production. Simulation of electromagnetism and thermomechanics, namely solving multiphysics, with the aid of commercial programs is possible by solving electromagnetism and thermomechanics separately. In other words the interaction between them is weakly introduced for enabling a computation. We want to present very briefly the method in [1, Chap. 3] solving all fields at once by incorporating the interaction accurately.

1 Weak form for multiphysics

The objective is to compute the temperature T in K(elvin), the displacement u_i in m(eter), the electric potential ϕ in V(olt), and the magnetic potential A_i in T(esla)m as functions in space x_i and time t. We neglect geometric nonlinearities such that x_i indicates the particle. The unknown fields $\{T, u_i, \phi, A_i\}$ are expressed in Cartesian coordinates, we use summation convention over repeated indices, and $_{,i}$ is used for partial derivative in x_i. For details of deriving the weak form, we refer to [2]. Basically, we use a governing equation for all fields: for the temperature by means of the balance of entropy, for the displacement with the balance of (linear) momentum, as follows

$$\rho\frac{\partial\eta}{\partial t}+\Phi_{i,i}-\rho\frac{r}{T}=\Sigma\ ,\quad \rho\frac{\partial^2 u_i}{\partial t^2}+\epsilon_{ijk}\frac{\partial\mathfrak{D}_j B_k}{\partial t}-(\sigma_{ji}+m_{ji})_{,j}-\rho f_i=0\ , \tag{1}$$

where the mass density ρ, the heat supply r, and the body force f_i are known; the free charge potential $\mathfrak{D}_i$, the free current potential $\mathfrak{H}_i$, and Maxwell's stress read

$$m_{ji}=-\frac{1}{2}\delta_{ji}(H_kB_k+D_kE_k)+H_iB_j+D_jE_i\ ,\quad \mathfrak{D}_i=D_i+P_i\ ,\quad \mathfrak{H}_i=H_i-\mathcal{M}_i\ , \tag{2}$$

with the Maxwell–Lorentz aether relations: $D_i=\varepsilon_0E_i$ and $H_i=\mu_0^{-1}B_i$. We need constitutive relations for the specific entropy η, for the entropy flux Φ_i, for the entropy production

Σ, for CAUCHY's stress σ_{ij}, for electric polarization P_i, and for magnetic polarization $\mathcal{M}_i$. Electromagnetic potentials are introduced,

$$E_i = -\phi_{,i} - \frac{\partial A_i}{\partial t} \ , \ B_i = \epsilon_{ijk} A_{k,j} \ , \tag{3}$$

by fulfilling two of four MAXWELL equations motivated by the FARADAY law. The other two of four MAXWELL equations are used in combination with the LORENZ gauge in order to obtain

$$\begin{aligned} \frac{\partial \mathfrak{D}_{i,i}}{\partial t} + \left(\jmath_i^{\text{fr.}} + \frac{\partial u_i}{\partial t} \mathfrak{D}_{j,j} + \epsilon_{ijk} \mathcal{M}_{k,j} \right)_{,i} = 0 \ , \\ \varepsilon_0 \frac{\partial^2 A_i}{\partial t^2} - \frac{1}{\mu_0} A_{i,jj} = \jmath_i^{\text{fr.}} + \frac{\partial u_i}{\partial t} \mathfrak{D}_{j,j} + \frac{\partial P_i}{\partial t} + \epsilon_{ijk} \mathcal{M}_{k,j} \ , \end{aligned} \tag{4}$$

which are utilized to compute the electromagnetic potentials, ϕ, A_i, respectively. For the free electric current $\jmath_i^{\text{fr.}}$, we need a constitutive equation. By using the usual strategy of generating a residual from Eqs. (1), (4) by subtracting right side from the left side, multiplying the residual by an arbitrary test function of the same rank as residual, integrating by parts the terms already possessing a derivative of unknowns, we acquire the weak form $\mathrm{F} = \mathrm{F}_\phi + \mathrm{F}_{\boldsymbol{A}} + \mathrm{F}_{\boldsymbol{u}} + \mathrm{F}_T$ with

$$\begin{aligned} \mathrm{F}_\phi &= \int_\Omega \Big(-(\mathfrak{D}_i - \mathfrak{D}_i^0)\delta\phi_{,i} - \Delta t \jmath_i^{\text{fr.}} \delta\phi_{,i} - (u_i - u_i^0)\mathfrak{D}_{j,j}\delta\phi_{,i} - \Delta t \epsilon_{ijk}\mathcal{M}_{k,j}\delta\phi_{,i} \Big) \,\mathrm{d}V + \\ &\quad + \int_{\Omega^I} N_i \Delta t \epsilon_{ijk} [\![\mathcal{M}_{k,j}]\!] \delta\phi \,\mathrm{d}A \ , \\ \mathrm{F}_{\boldsymbol{A}} &= \int_\Omega \Bigg(\varepsilon_0 \frac{A_i - 2A_i^0 + A_i^{00}}{\Delta t^2} \delta A_i + \frac{1}{\mu_0} A_{i,j} \delta A_{i,j} - \jmath_i^{\text{fr.}} \delta A_i - \frac{u_i - u_i^0}{\Delta t} \mathfrak{D}_{j,j} \delta A_i - \\ &\quad - \frac{P_i - P_i^0}{\Delta t} \delta A_i + \epsilon_{ijk} \mathcal{M}_k \delta A_{i,j} \Bigg) \,\mathrm{d}V \ , \\ \mathrm{F}_{\boldsymbol{u}} &= \int_\Omega \Bigg(\rho \frac{u_i - 2u_i^0 + u_i^{00}}{\Delta t^2} \delta u_i + \epsilon_{ijk} \frac{\mathfrak{D}_j B_k - \mathfrak{D}_j^0 B_k^0}{\Delta t} \delta u_i - \bar{\sigma}_{ji,j} \delta u_i + \tau_{ji} \delta u_{i,j} - \\ &\quad - \rho f_i \delta u_i \Bigg) \,\mathrm{d}V + \int_{\partial\Omega^I} N_j [\![\bar{\sigma}_{ji}]\!] \delta u_i \,\mathrm{d}A + \int_{\partial\Omega^N} (\hat{t}_i - N_j \bar{\sigma}_{ji}) \delta u_i \,\mathrm{d}A \ , \\ \mathrm{F}_T &= \int_\Omega \left(\rho(\eta - \eta^0)\delta T - \Delta t \Phi_i \delta T_{,i} - \Delta t \rho \frac{r}{T} \delta T - \Delta t \Sigma \delta T \right) \mathrm{d}V \ , \end{aligned} \tag{5}$$

discretely in time with Δt being the time step and $(\cdot)^0$ denoting the numerical value computed at the last instant, after implementing the balance equations on singular surfaces in order to incorporate the jump terms on interfaces $\partial\Omega^I$ with its outward normal N_i between different materials, see [2, Sect. 4]. We also incorporated the so-called NEUMANN boundaries $\partial\Omega^N$ for implementing the given traction stress $\hat{t}_i$ in the following application.

2 Constitutive relations for an elastic, piezoelectric, linear material

Consider a linear, piezoelectric but non-magnetized, $\mathcal{M}_i = 0$, material with the following constitutive equations for reversible processes obtained by a thermodynamical analysis

$$\begin{aligned} \eta = c \ln\left(\frac{T}{T_{\text{ref.}}}\right) + \mathrm{v} C_{ijkl} \alpha_{kl} \varepsilon_{ij} - \mathrm{v} \tilde{T}_{ijk} \alpha_{jk} E_i \ , \quad \sigma_{ij}^{\text{tot.}} = \sigma_{ij} + m_{ij} = \bar{\sigma}_{ij} + \tau_{ij} \ , \\ \bar{\sigma}_{ij} = -C_{ijkl} \alpha_{kl} (T - T_{\text{ref.}}) \ , \quad \tau_{ij} = m_{ij} + P_i E_j + C_{ijkl} \varepsilon_{kl} - \tilde{T}_{kij} E_k \ , \\ P_i = -\tilde{T}_{ijk} \alpha_{jk} (T - T_{\text{ref.}}) + \tilde{T}_{ijk} \varepsilon_{jk} + \varepsilon_0 \chi_{ij}^{\text{el.}} E_j \ , \end{aligned} \tag{6}$$

where $\mathrm{v} = \rho^{-1}$ and the material constants: stiffness tensor C_{ijkl}, thermal expansion coefficients α_{ij}, piezoelectric tensor $\tilde{T}_{ijk} = C_{jklm} \tilde{d}_{ilm}$ given by the piezoelectric coefficients $\tilde{d}_{ijk}$, electric

susceptibility $\chi_{ij}^{\text{el.}}$ are determined by experiments. They are all constants, otherwise the above equations would be incorrect. In other words, we neglect hyperelasticity and electrostriction. Moreover, by neglecting irreversible deformation (neither viscoelasticity nor plasticity exists) and irreversible polarization (no hysteresis), we obtain

$$\begin{gathered}\Phi_i = \frac{q_i}{T}\ ,\ \Sigma = -\frac{q_i}{T^2}T_{,i} + \frac{1}{T}\mathcal{E}_i \jmath_i^{\text{fr.}}\ ,\ \mathcal{E}_i = E_i + \epsilon_{ijk}\frac{\partial u_j}{\partial t}B_k\ , \\ q_i = -\kappa T_{,i} + \varsigma\pi T\mathcal{E}_i\ ,\ \jmath_i^{\text{fr.}} = \varsigma\pi T_{,i} + \varsigma\mathcal{E}_i\ ,\end{gathered} \tag{7}$$

with the material parameter: thermal conductivity κ, electrical conductivity ς, and thermoelectric constant π. For simplicity we assume that these material parameters are constant. For detailed discussion and derivation of these constitutive relations, we refer to [1, Chap. 3].

3 Simulation of a piezoelectric pressure sensor

A thin metal membrane disk bends under a dynamic pressure. A piezoelectric thicker disk is attached on its bottom side to the membrane and it is clamped on its upper side as shown in Figure 1. Deformation of the piezoelectric disk is measured as a voltage drop, which, after calibrating with a known pressure change, measures the dynamic pressure. Such a sensor is used to measure the dynamic pressure in engine combustion and ballistic. Due to the voltage leak in connectors, a static pressure is difficult with this sensor. We model part of the case as steel and the piezoelectric disk as a PZT-5H ceramic with the materials data compiled in Table 1. The

Table 1. Material constants used in the simulation for the stainless steel as the case, PZT-5H as the piezoelectric disk, and the surrounding air

		Steel	PZT-5H	Air
Mass density	ρ in kg/m^3	8500	7500	1.2
Compliance	S_{33} in m^2/N	$4.8 \cdot 10^{-12}$	$20 \cdot 10^{-12}$	1
	S_{11} in m^2/N	$4.8 \cdot 10^{-12}$	$15.6 \cdot 10^{-12}$	1
Poisson's ratio	ν	0.31	0.31	0
Piezoelectric constants	$\tilde{d}_{33}$ in m/V	0	$585 \cdot 10^{-12}$	0
	$\tilde{d}_{31}$ in m/V	0	$-265 \cdot 10^{-12}$	0
	$\tilde{d}_{15}$ in m/V	0	$730 \cdot 10^{-12}$	0
Dielectric constants	$\bar{\varepsilon}_{33}^{\text{el.}}$	1	3400	1
	$\bar{\varepsilon}_{11}^{\text{el.}}$	1	3130	1
Specific heat capacity	c in J/(kg K)	390	350	0
Coefficients of thermal expansion	α_{33} in K^{-1}	$12 \cdot 10^{-6}$	$-4 \cdot 10^{-6}$	$3.43 \cdot 10^{-3}$
	α_{11} in K^{-1}	$12 \cdot 10^{-6}$	$6 \cdot 10^{-6}$	$3.43 \cdot 10^{-3}$
Thermal conductivity	κ in W/(m K)	16	1.1	$2.6 \cdot 10^{-2}$
Thermoelectric constant	π in V/K	$60 \cdot 10^{-6}$	0	0
Electric conductivity	ς in S/m	10^6	0	0

compliance matrix, S_{IJ}, in Voigt's notation,

$$S_{IJ} = \begin{pmatrix} S_{11} & -\nu S_{11} & -\nu S_{11} & 0 & 0 & 0 \\ -\nu S_{11} & S_{11} & -\nu S_{11} & 0 & 0 & 0 \\ -\nu S_{11} & -\nu S_{11} & S_{33} & 0 & 0 & 0 \\ 0 & 0 & 0 & (1+\nu)S_{11} & 0 & 0 \\ 0 & 0 & 0 & 0 & (1+\nu)S_{11} & 0 \\ 0 & 0 & 0 & 0 & 0 & (1+\nu)S_{11} \end{pmatrix}\ , \tag{8}$$

is the inverse of the stiffness matrix in VOIGT's notation such that we obtain $C_{IJ} = (S_{JI})^{-1}$. Analogously, we have the piezoelectric constants, $\tilde{d}_{iJ}$, where VOIGT's notation is applied on the indices belonging to the strain,

$$\tilde{d}_{iJ} = \begin{pmatrix} \tilde{d}_{111} & \tilde{d}_{122} & \tilde{d}_{133} & \tilde{d}_{123} & \tilde{d}_{131} & \tilde{d}_{112} \\ \tilde{d}_{211} & \tilde{d}_{222} & \tilde{d}_{233} & \tilde{d}_{223} & \tilde{d}_{231} & \tilde{d}_{212} \\ \tilde{d}_{311} & \tilde{d}_{322} & \tilde{d}_{333} & \tilde{d}_{323} & \tilde{d}_{331} & \tilde{d}_{312} \end{pmatrix} = \begin{pmatrix} 0 & 0 & 0 & 0 & \tilde{d}_{15} & 0 \\ 0 & 0 & 0 & \tilde{d}_{15} & 0 & 0 \\ \tilde{d}_{31} & \tilde{d}_{31} & \tilde{d}_{33} & 0 & 0 & 0 \end{pmatrix} . \tag{9}$$

The susceptibility is given by the relative permittivity values:

$$\chi^{\text{el.}}_{ij} = \begin{pmatrix} \bar{\varepsilon}^{\text{el.}}_{11} & 0 & 0 \\ 0 & \bar{\varepsilon}^{\text{el.}}_{11} & 0 \\ 0 & 0 & \bar{\varepsilon}^{\text{el.}}_{33} \end{pmatrix} - \delta_{ij} \ . \tag{10}$$

We code in Python and use FEniCS [3] for solving the system of equations. In Figure 1 the input pressure and the system response is seen. The real outcome is more than visualized, we acquire 3D deformation, temperature, and electromagnetic fields.

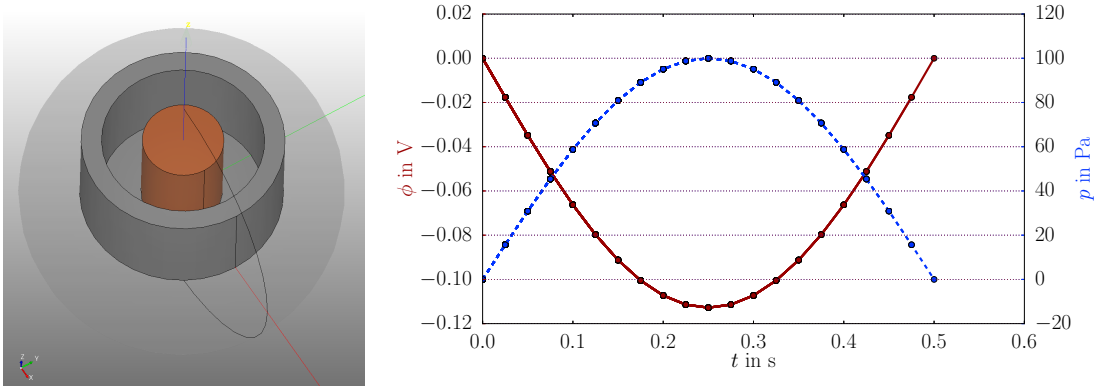

Figure 1. Left: CAD geometry of a stainless steel case with a thin membrane (gray) and an attached piezoelectric disk (red), embedded in air (transparent gray). Right: Input and output of this system as a transient solution of the coupled and nonlinear weak form.

Conclusions

We have applied a solution strategy for MEMS, where all thermodynamical fields are solved at once. This strategy is indeed important for a coupled system, especially in MEMS the coupling is the key of the mechanism such that we need to simulate a system with the highest precision in the coupling terms. Moreover, the system is nonlinear—caused by the entropy production. Therefore, we omit a method based on splitting and solving the equations subsequently. Instead, we use the novel open-source packages developed under the FEniCS project and solve all equations together. A common example from the industry, a dynamical piezoelectric pressure sensor is presented in order to uncover the versatility of the proposed solution strategy.

References

[1] B. E. Abali. *Computational Reality, Solving Nonlinear and Coupled Problems in Continuum Mechanics*. Advanced Structured Materials. Springer, 2016.

[2] B. E. Abali and F. A. Reich. Thermodynamically consistent derivation and computation of electro-thermo-mechanical systems for solid bodies. *Computer Methods in Applied Mechanics and Engineering*, pages –, 2017.

[3] J. Hoffman, J. Jansson, C. Johnson, M. Knepley, R. Kirby, A. Logg, L. R. Scott, and G. N. Wells. FEniCS. http://www.fenicsproject.org/, 2005.